Macrothink Institute™

International Journal of Civil Aviation
ISSN 1943-3433
2009, Vol. 1, No. 1: E5

Realistic Speed Change Maneuvers for Air Traffic Conflict Avoidance and their Impact on Aircraft Economics

Cem Cetek,Phd

Assistant Professor

School of Civil Aviation, Anadolu University

Iki Eylul Kampusu, 26460, Eskisehir, Turkey

Tel: +90-222-322 20 ext.6936 E-mail: ccetek@anadolu.edu.tr

Abstract

Sharp increase in air traffic densities in the world over the last decade made many researchers prompted to investigate innovative air traffic management concepts to improve the current air traffic capacity and economic performance of aircraft. Providing aircraft operators more freedom to choose their trajectories is one of them. In such an air traffic environment, resolution of aircraft conflicts is a key element for both flight safety and aircraft economics.

This study analyzes the economic performance of a specific conflict resolution strategy based on speed change between two aircraft in terms of extra time and fuel consumption. In this strategy, minimum time solutions are investigated without violating safe separation and realistic operational constraints for various flight and conflicts conditions in horizontal plane. Maneuver models include detailed aerodynamic and engine characteristics to make a more accurate analysis, which is very critical for both safety and economic efficiency concerns.

Using speed change alone seems unattractive since it requires longer resolution time than heading change. On the other hand, speed change maneuvers can support heading change maneuvers and extend their range of application especially for small route crossing angles. Study of such isolated conflict resolution cases can be an effective tool for both aircraft operators and air traffic system designers to make a complete economic performance analysis of flight in possible future scenarios.

Keywords: Aircraft Economics, Air Traffic Control, Conflict Resolution, Trajectory Optimization

1. Introduction

Number of the civil flights increased over 40% in the last decade all over the western world (Eurocontrol, 2008a). Various projections for the next ten years show that the demand for air transportation will grow at about 30-47% (Eurocontrol, 2008b). These numbers indicate that the problems of the current ATM system regarding capacity and efficiency will become much more serious in the future.

In order to overcome these problems, researchers have been working on innovative ATM concepts such as free flight, providing more freedom to aircraft operators to choose their trajectories (RTCA, 2005). In such a flexible air traffic environment, resolution of aircraft conflicts is a key element for both flight safety and aircraft economics.

There are numerous studies regarding conflict resolution from both algorithmic and operational perspectives. Most of these approaches are summarized in (Kuchar & Yang, 2000; Dimarogonas & Kyriakopoulous, 2003; Mendoza, 1999, Eurocontrol, 2002). Despite this extensive literature, studies investigating conflict resolution maneuvers in terms of aircraft economics are still limited in number and context with few exceptions (Valenti Clari et al., 2002; Krozel & Peters, 1997).

The aim of this study is to analyze the economic performance of a specific conflict resolution strategy based on speed change maneuvers. This strategy includes non-cooperative avoidance and recovery maneuvers between two aircraft in the horizontal plane. In the analysis, minimum time solutions for resolution and recovery are investigated for various flight and conflict scenarios. Delays and extra fuel consumption are calculated for the each case with respect to the reference flight conditions. Maneuvers subjected realistic operational constraints include more detailed aerodynamic and engine models for an accurate analysis.

2. Mathematical Model

2.1 Problem Statement

Air traffic conflict arising between two commercial aircraft at the same flight altitude with intersecting routes is shown in Figure 1. Their encounter geometry can be characterized by their relative linear and angular positions as

$$\theta = \psi_1(t) - \psi_2 \tag{1}$$

$$s(t) = \left((x_1(t) - x_2(t))^2 + y_1^2(t)\right)^{1/2} \tag{2}$$

In (1), θ is the path crossing angle; and ψ_1, ψ_2 are the headings of the aircraft 1 and 2, respectively. In (2), s is the distance between the aircraft; and x_1, y_1 and y_2 are linear positions of the aircraft. The ratio of initial airspeeds of the aircraft is described as

$$VR = \frac{v_{20}}{v_{10}} \tag{3}$$

In (3), v_{10}, v_{20} are the airspeeds of the aircraft at time, $t = t_0$. The closest distance between the aircraft, s_{min} is another parameter indicating the seriousness of the conflict. For en route airspace any encounter results in conflict $0 \leq s_{min} < s_y$ for any $t \in [\, t_0 \,, t_f]$ where s_y is the minimum horizontal safe separation and equals to 9.26 km (5nm).

It is supposed that if no avoidance action is taken, at t_c, aircraft 1 will reach point C whereas the aircraft 2 will be at point C'. Let the distance $s' = |\, CC' \,|$, can be calculated in terms of VR, θ and s_{min} as

$$s' = s_{\min}\left(\left(1-\frac{(VR-\cos\theta)^2}{VR^2-2VR\cos\theta+1}\right)^2+\left(\frac{(VR-\cos\theta)\sin\theta}{VR^2-2VR\cos\theta+1}\right)^2\right)^{-1/2} \tag{4}$$

where the distances $|\, OC \,|$ and $|\, OC' \,|$ are unknowns. They will be determined using an optimization process in part 3. The time t_c can be found using the following relation:

$$t_c = \frac{|OC|}{v_{10}} = \frac{|OC'|+s'}{VRv_{10}} \tag{5}$$

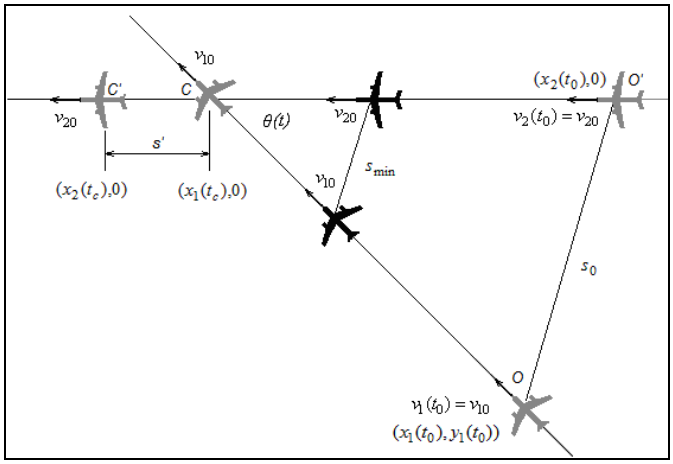

Figure 1. Conflict geometry of the aircraft with intersecting linear routes.

2.2 *Rules of Road*

Since non-cooperative conflict resolution is investigated, a set of rules of road is necessary. The following assumptions are made as the rules of road in the encounter described in Figure 1.

1. $VR \geq 1$
2. No overtaking or head-on encounter is considered.
3. Slower aircraft is always supposed to maneuver.
4. If the airspeeds are equal, the aircraft on the starboard has the road priority.

According to these assumptions, aircraft 1 always maneuvers, while aircraft 2 takes no action.

2.2 *Equations of Motion*

The following point mass equations of motion are used to describe the system shown in Fig. 1.

$$\dot{x}_1 = a(\sigma)M_1(t)\cos\theta(t) \tag{6}$$

$$\dot{y}_1 = a(\sigma)M_1(t)\sin\theta(t) \tag{7}$$

$$\dot{x}_2 = a(\sigma)\cdot VR\cdot M_1(t_0) \tag{8}$$

$$\dot{M}_1 = \frac{1}{m_1\cdot a(\sigma)}(\eta_1 F_1(\sigma, M_1) - D_1(\sigma, M_1, \alpha_1) \tag{9}$$

$$L(\sigma, M_1, \alpha_1) - m_1 g = 0 \tag{10}$$

where a is the speed of sound; σ is the relative density at the given flight altitude; g is the gravitational acceleration; $M_1=v_1/a(\sigma)$ is the Mach number; m_1 is the reference mass; F_1 is the nominal engine thrust; D_1 is the aerodynamic drag force; η_1 is the throttle setting and α_1 is the angle of attack of the aircraft 1. Equations (6)-(10) are derived assuming standard atmospheric conditions, zero wind, constant mass and small angle of attack controlling aircraft to maintain the flight altitude constant.

For horizontal flight, aerodynamic drag force, D on the aircraft including effects of compressibility and cambered wing can be formulated as

$$D_1(M) = d_1 M_1^{\,2} + \frac{d_2 M_1^{\,2}}{\sqrt{1 - M_1^{\,2}}}\left(\frac{d_3}{M_1^{\,2}} - d_4\right)^2 \tag{11}$$

where d_1,d_2, d_3 and d_4 drag force parameters depending on flight level and aircraft's physical and aerodynamic properties. Total nominal engine thrust, F_1 is modeled based on a high by-pass ratio gas turbofan jet engine data from (McCormick, 1979) as

$$F(\sigma, M) = c_1 M_1^{\,2} + c_2 M_1 + c_3 \tag{12}$$

where c_1, c_2 and c_3 are thrust parameters as a function of flight level. The system described in (6)-(10) is subjected to the following constraints in [t_0 ,t_f]

$$s(t) \geq s_y \tag{13}$$

$$M_{1md} \leq M_1 \leq M_{10} = M_{cr} \tag{14}$$

In (14), M_{1md} is the minimum drag Mach number, and M_{cr} is the optimal cruise Mach number for fuel consumption at the chosen flight altitude. The control variable, η_1 is also limited by the following operational constraints

$$\eta_{\min} \leq \eta_1 \leq \eta_{\max} \tag{15}$$

These minimum and maximum throttle setting values depend on the following acceleration

limits imposed by passenger comfort limits (Nuic, 2003) and engine constraints such that

$$-0.02g \le a_{\min} \le \dot{v}_1 \le a_{\max} \le 0.02g \tag{16}$$

The accuracy of the point mass model described in (6)-(10) can be increased if throttle setting transients are taken into account. Transient changes in $\Delta\eta_1$ can be described using a first-order response model described as (Etkin & Reid, 1996)

$$\Delta\eta_1 = \Delta\eta_1^c(1 - e^{(-t/\tau_c)}) \tag{17}$$

where $\Delta\eta_1^c$ is the throttle command and τ_c is the time constant which is taken as 3.5 seconds. From Figure 1, initial conditions of the system are described as

$$(x_1(t_0), y_1(t_0)) = (|OC|\cos\theta, |OC|\sin\theta) \tag{18}$$

$$(x_2(t_0), y_2(t_0) = (|O'C|, 0) \tag{19}$$

$$v_1(t_0) = v_{10} = v_{cr} \tag{20}$$

$$v_2(t_0) = v_{20} = VR \cdot v_{cr} \tag{21}$$

Final conditions are defined from Figure 2 as follows:

$$(x_1(t_f), y_1(t_f)) = (|CD|\cos\theta, |CD|\sin\theta) \tag{22}$$

$$(x_2(t_0), y_2(t_0) = (|CD'|, 0) \tag{23}$$

$$v_1(t_0) = v_{10} = v_{cr} \tag{24}$$

$$v_2(t_0) = v_{20} = VR \cdot v_{cr} \tag{25}$$

In (18)-(25), t_0=0 and distances | OC |, | OC' |, | CD | and | CD'| depend on free final time, t_f.

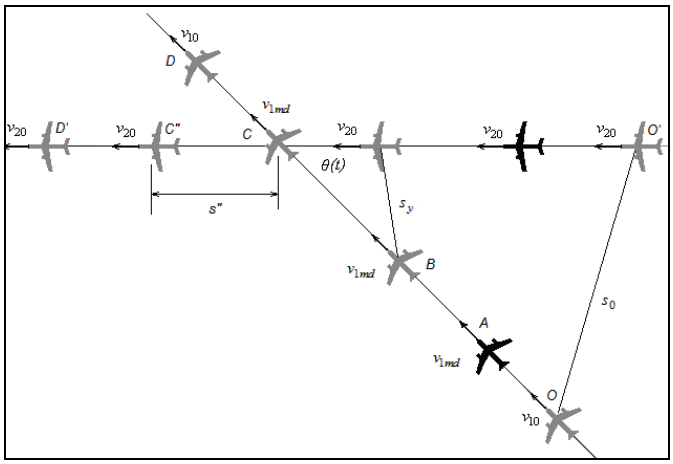

Figure 2. Non-cooperative speed change avoidance and recovery maneuvers.

3. Resolution Strategy

3.1 Speed Change Maneuvers

Speed change strategy is graphically described in Fig. 2. In order to perform speed maneuvers in minimum time with satisfying the constraints (13)-(16) and boundary conditions (18)-(25), a three step procedure is proposed. These steps are slowing down with maximum deceleration (from point O to A), steady flight at the minimum allowable speed (from point A to C) and speeding up back to the original speed with maximum acceleration (from point C to D). Total resolution (avoidance and recovery) time, therefore, can be described as

$$t_f = T_{dec} + T_{ss} + T_{acc} \tag{26}$$

where T_{dec} is the period of deceleration in $[t_0,t_1]$; T_{ss} is the period of cruise at the minimum speed in $[t_1,t_2]$ and T_{acc} is the period of acceleration back to the original speed in $[t_2,t_3]$. T_{dec} and T_{acc} can be formulated with the following relations

$$T_{dec} = \frac{a(\sigma)\left|M_{cr} - M_{md}\right|}{\left|\dot{v}_1\right|_{t_0}^{t_1}} = \frac{a(\sigma)\left|M_{cr} - M_{md}\right|}{\left|a_{\min}\right|} + t_{thrt} \tag{27}$$

$$T_{acc} = \frac{a(\sigma)\left|M_{cr} - M_{md}\right|}{\left|\dot{v}_1\right|_{t_2}^{t_3}} = \frac{a(\sigma)\left|M_{cr} - M_{md}\right|}{\left|a_{\max}\right|} + t_{thrt} \tag{28}$$

In (27)-(28), the term, t_{thrt} is the delay due to throttle setting transients described in (17). Using the conflict geometries before and after the resolution in Figure 1 and Figure 2, T_{ss} can be described as

$$T_{ss} = \frac{\left|OA\right| / v_{10} + (s'' - s') / (VR \cdot v_{10}) - T_{dec}}{(1 - v_{1md} / v_{10})} \tag{29}$$

The distance $|\,OA\,|$ can be calculated using the following relation

$$|OA| = \int_0^{T_{dec}} \dot{v}_1(t)dt \tag{30}$$

The only unknown parameter in (29) is the distance *s"* and in order to find it, the following constrained optimization problem is supposed to be solved.

$$\min\left(\left((v_2^0 - v_{1md}\cos\theta)\tau - s''\right)^2 + \left(v_{1md}\sin\theta\cdot\tau\right)^2 - s_y^2\right) \tag{31a}$$

$$s(\tau) \geq s_y \tag{31b}$$

$$s'' \geq s_y \tag{31c}$$

In (31), τ=t-t_1.

3.2 Reference Time and Fuel Consumption

During the resolution process, aircraft 1 flies the distance $|CD|$. Reference time is calculated based on this distance as

$$t_{ref} = \frac{|OD|}{v_{10}} \tag{32}$$

Therefore, the delay due to the maneuvers can be written as

$$\Delta t = t_f - \frac{|OD|}{v_{10}} \tag{33}$$

In order to calculate fuel consumption, fuel flow rate of the engines should be known. Based on the engine data [13], fuel flow rate is modeled as a quadratic function of η_1 as

$$\dot{\omega}_f = (f_1(\sigma, M_1)\eta_1^2 + f_2(\sigma, M_1)) \cdot F_1(\sigma, M) \tag{34}$$

In (34), f_1 and f_2 are fuel flow parameters and can be written as a function of Mach number as

$$f_1(M_1) = a_1 M_1^2 + a_2 M_1 + a_3 \tag{35}$$

$$f_2(M_1) = b_1 M_1^2 + b_2 \tag{36}$$

In (35)-(36), a_1, a_2, a_3, b_1 and b_2 are specific fuel consumption (SPC) constants for the given flight altitude. Therefore, reference and extra fuel consumptions are as follows

$$(\omega_f)_{ref} = \int_0^{t_{ref}} \dot{\omega}_f dt \tag{37}$$

$$\Delta\omega_f = \omega_f - (\omega_f)_{ref} \tag{38}$$

4. Results

4.1 Simulation Parameters

Resolution maneuvers are tested for a narrow body commercial jet transport based on Boeing 737-400 physical and aerodynamic data in Gong & Chan (2002) and Etkin & Reid (1996). Thrust and specific fuel consumption data in McCormick (1979) is adapted for this aircraft. In calculations *VR* are limited in between 1.0 and 1.4. For commercial jet transports, it seems unlikely to have *VR* values greater than 1.4, while they flight at their optimal cruise speed in en route airspace.

As it is mentioned earlier, no head-on or overtaking conflicts are considered in the study; therefore, values of the path crossing angle, θ are taken in between 30˚and 150˚in the analysis. Minimum horizontal separation before the resolution, s_{min} is set to 0, 3.7 and 7.4 km (0, 2 and 4 nm) during the tests. Simulation parameters regarding aircraft model and flight conditions are listed in Table 1.

Table 1. Simulation parameters used in the analysis

Parameter		Value
h	Altitude, m (ft)	7600 (25000)
M_{md}	Minimum Drag Mach Number	0.572
M_{cr}	Optimum Cruise Mach Number	0.645
m	Mass of Aircraft (kg)	58,000
d_1	Drag Constant (N)	62,338
d_2	Drag Constant (N)	122,390
d_3	Drag Constant	0.2372
d_4	Drag Constant	0.2
c_1	Thrust Constant (N)	32,504
c_2	Thrust Constant (N)	-46,086
c_3	Thrust Constant (N)	78,720
a_1	SPC constant (kg/N/s)	$1.698 \cdot 10^{-5}$
a_2	SPC constant (kg/N/s)	$-2.038 \cdot 10^{-5}$
a_3	SPC constant (kg/N/s)	$0.699 \cdot 10^{-5}$
b_1	SPC constant (kg/N/s)	$0.976 \cdot 10^{-5}$
b_2	SPC constant (kg/N/s)	$1.023 \cdot 10^{-5}$

4.2 Test Results

During the simulations, total resolution time; total time delay and percentage extra fuel consumption are estimated for the given conflict configurations. In each test, variations of these measures with respect to θ, *VR* and s_{min} are analyzed. Simulation code is written using Optimization Toolbox of MATLAB software.

In Figure 3, variation of total resolution (avoidance and recovery) time, t_f with θ is shown for VR=1.0, 1.2 and 1.4, respectively. For the smaller values of θ, t_f is about 11 minutes and VR

has no significant effect on it. As θ increases, t_f reaches to unacceptable values for the deterministic conflict resolution. Higher values of VR result in shorter t_f, especially when $\theta \geq 60^{\circ}$.

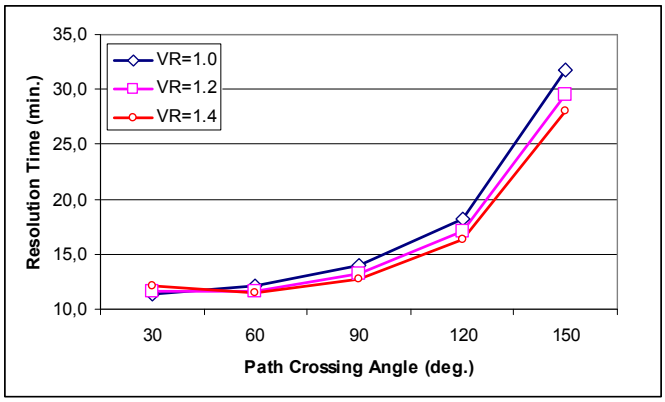

Figure 3. Variation of the total resolution (avoidance and recovery) time with path crossing angle and initial speed ratio of the aircraft.

Pre-solution minimum horizontal separation, effect of s_{min} on t_f is stronger than VR, as it can be seen from Figure 4. As s_{min} decreases, naturally the conflict becomes more dangerous and longer t_f is required for resolution. For larger values of s_{min}, t_f becomes less sensitive to the variation of θ.

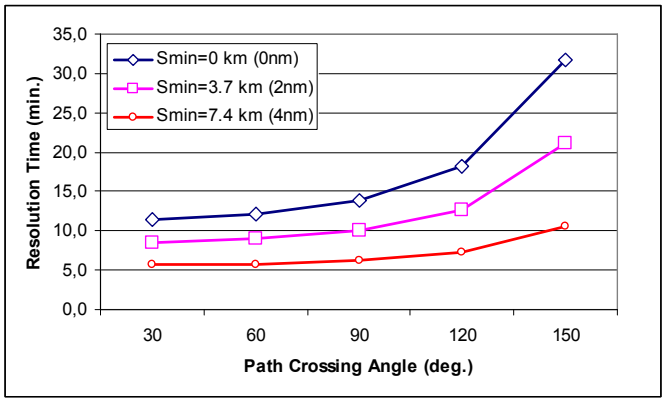

Figure 4. Variation of the total resolution (avoidance and recovery) time with path crossing angle and minimum horizontal separation before the resolution.

Similar to t_f, time delay increases drastically with increasing θ (Figure 5 and 6). For $\theta < 90^{\circ}$, it is under 60 seconds, which proves that speed change is effective for the encounters having narrow crossing angles.

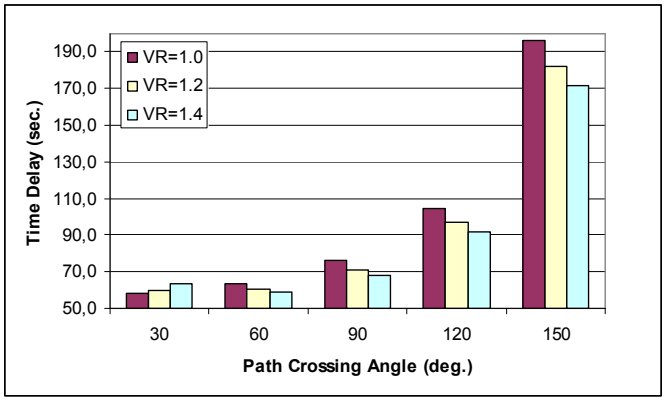

Figure 5. Variation of total time delay with path crossing angle and initial speed ratio of the aircraft.

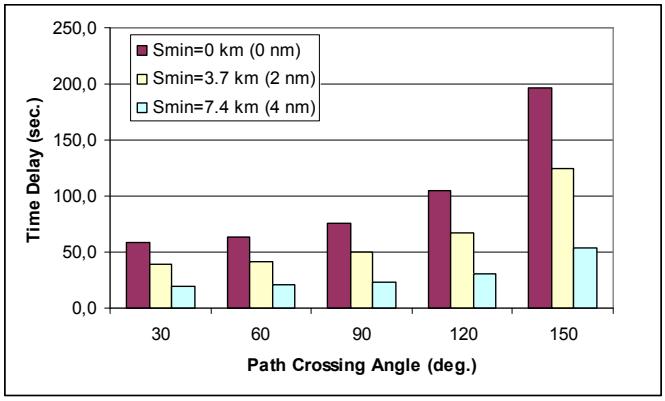

Figure 6. Variation of total time delay with path crossing angle and minimum horizontal separation before the resolution.

Figure 7 and 8 show that percentage extra fuel consumption is not as sensitive as time delay to the variation of θ, *VR* and s_{min}. It remains at about 3% in most of the cases. Therefore, in terms of total cost, speed change maneuvers are less costly for smaller crossing angles.

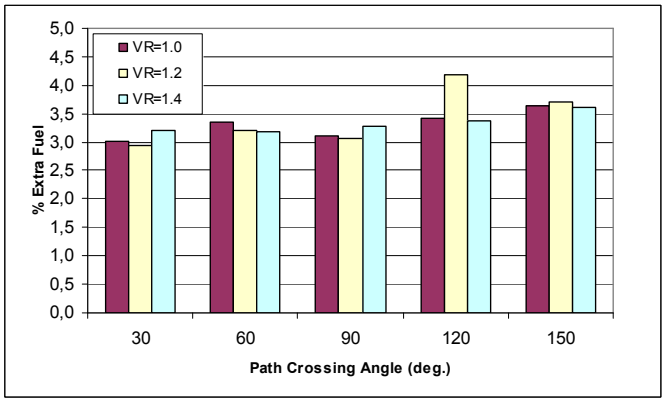

Figure 7. Variation of % extra fuel consumption with path crossing angle and initial speed ratio of the aircraft.

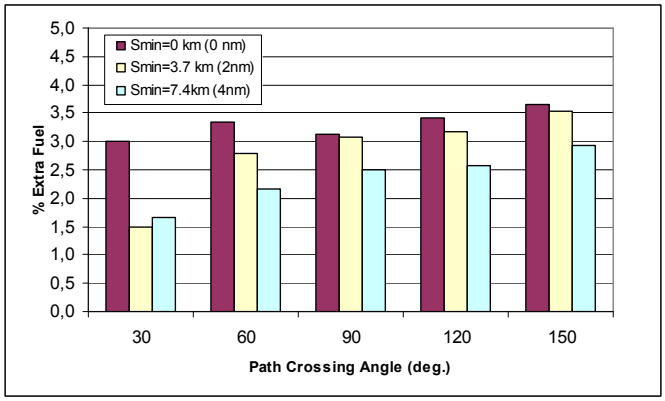

Figure 8. Variation of % extra fuel consumption with path crossing angle and minimum horizontal separation before the resolution.

5. Conclusion

Minimum time speed change maneuvers have a certain drawback regarding the total resolution time. It takes longer to resolve a conflict especially when the routes of the aircraft intersect with large angles. Therefore using the speed changes for the conflict resolution alone is less preferable than heading changes. On the other hand, it can be helpful to use them combined with heading maneuvers. For the crossing angles less than 90˚, significant cuts in time can be obtained using them. Combined use of speed and heading maneuvers may also help to use less lateral space and therefore increase the capacity of the airspace. These advantages make use of speed change maneuvers for the conflict resolution interesting.

Though this study on speed change strategies focuses on a very restricted case of conflict resolution, further investigation on this topic can provide essential tools for aircraft operators and air traffic system designers to make a more complete economic performance analysis of flight in possible future scenarios.

References

Dimarogonas, D. and Kyriakopoulous, K. (2003). Inventory of Decentralized Conflict Detection and Resolution Systems in Air Traffic, HYBRIDGE Task 6.1 v.2.0, IST-2001-32460 of European Commission.

Eurocontrol, (2002). Towards a Controller-based Conflict Resolution Tool-A Literature Review, CORA 2 Project, ASA.01.CORA2.DEL04-A.LIT, v.01, Brussels, Belgium.

Eurocontrol, (2008a). Medium-Term Forecast Flight Movements (2008-2014) Vol.1, STATFOR Doc280, Brussels, Belgium.

Eurocontrol, (2008b). Long-Term Forecast Flights (2008-2030) Vol.1, STATFOR Doc302, Brussels, Belgium.

Etkin, B. and Reid, L.D. (1996). *Dynamics of Flight-Stability and Control 3rd Edition*, Wiley and Sons Inc., Toronto, Canada.

Gong, C. and Chan, W.N. (2002) Using Flight Manual Data to Derive Aeor-Propulsive Models for Predicting Aircraft Trajectories, AIAA Aircraft Technology, Integration and Operations Conference, Los Angeles, USA.

Krozel, J. and Peters, M. (1997). Strategic Conflict Detection and Resolution for Free Flight, Proceedings of the Conference on Decision and Control, San Diego, USA.

Kuchar, J.K. and Yang, L.C.(2000). A Review of Conflict Detection and Resolution Modeling Methods, *IEEE Transactions on Intelligent Transportation Systems,* **1**, 179-189

Nuic, A. (2003).User Manual for the Base of Aircraft Data (BADA) Revision 3.5, Eurocontrol Experimental Center, ECC Note No. 11/03, Brétigny-sur-Orge CEDEX, France.

McCormick, (1979). B.W., *Aerodynamics, Aernautics, and Flight Mechanics*, J. Wiley, New York, USA.

Mendoza, M. (1999). Current State of ATC Conflict Resolution, Eurocontrol Experimental Center, ECC Note No. 12/99, Bretigny, France.

RTCA, (1995). Advancing Free Flight Through Human Factors, Technical Workshop Report, FAA AAR-100.

Valenti Clari, M.S.V, Ruigrok, R.C.J., Heesbeen, B.W.M. and Groeneweg, J. (2002). Research Flight Simulation of Future Autonomous Aircraft Operations, Proceedings of Winter Simulation Conference, San Diego, USA .